HHS Public Access

Author manuscript

J Proteome Res. Author manuscript; available in PMC 2016 April 28.

Published in final edited form as:

J Proteome Res. 2015 April 3; 14(4): 1810–1817. doi:10.1021/pr5011923.

Comparison of GC-MS and GC×GC-MS in the Analysis of Human Serum Samples for Biomarker Discovery

Jason H. Winnike[⊥,¶], **Xiaoli Wei**[†,¶], **Kevin J. Knagge**[⊥], **Steven D. Colman**[⊥], **Simon G. Gregory**[⊥,‡], and **Xiang Zhang**[†,*]

[⊥]David H. Murdock Research Institute, Kannapolis, North Carolina 28081, United States

[†]Departments of Chemistry, Pharmacology & Toxicology, Center for Regulatory and Environmental Analytical Metabolomics (CREAM), University of Louisville, Louisville, Kentucky 40292, United States

[‡]Duke Molecular Physiology Institute, Department of Medicine, Duke University, Durham, North Carolina 27701, United States

Abstract

We compared the performance of gas chromatography time-of-flight mass spectrometry (GC-MS) and comprehensive two-dimensional gas chromatography mass spectrometry (GC×GC-MS) for metabolite biomarker discovery. Metabolite extracts from 109 human serum samples were analyzed on both platforms with a pooled serum sample analyzed after every 9 biological samples for the purpose of quality control (QC). The experimental data derived from the pooled QC samples showed that the GC×GC-MS platform detected about three times as many peaks as the GC-MS platform at a signal-to-noise ratio SNR ≥ 50, and three times the number of metabolites were identified by mass spectrum matching with a spectral similarity score $R_{sim} \geq 600$. Twenty-three metabolites had statistically significant abundance changes between the patient samples and the control samples in the GC-MS data set while 34 metabolites in the GC×GC-MS data set showed statistically significant differences. Among these two groups of metabolite biomarkers, nine metabolites were detected in both the GC-MS and GC×GC-MS data sets with the same direction and similar magnitude of abundance changes between the control and patient sample groups. Manual verification indicated that the difference in the number of the biomarkers discovered using these two platforms was mainly due to the limited resolution of chromatographic peaks by the GC-MS platform, which can result in severe peak overlap making subsequent spectrum deconvolution for metabolite identification and quantification difficult.

[*]**Corresponding Author**. Phone: +01 502 852 8878. Fax: +01 502 852 8149. xiang.zhang@louisville.edu.

[¶]These two authors contributed equally to this study.

ASSOCIATED CONTENT

Supporting Information

Figure S1: PLSDA analysis of the metabolite profiles of all patient samples. Figure S2: Abundance distribution of metabolite 5 between the control and the patient samples. Table S1: Data processing parameters used in LECO ChromaTOF. Table S2: Metabolite peaks detected by the GC-MS platform as potential biomarkers that have significant abundance differences between the patient and control samples. Table S3: Metabolite peaks detected by the GC×GC-MS platform as potential biomarkers that have significant abundance differences between the patient and control samples. This material is available free of charge via the Internet at http://pubs.acs.org.

The authors declare no competing financial interest.

Graphical Abstract

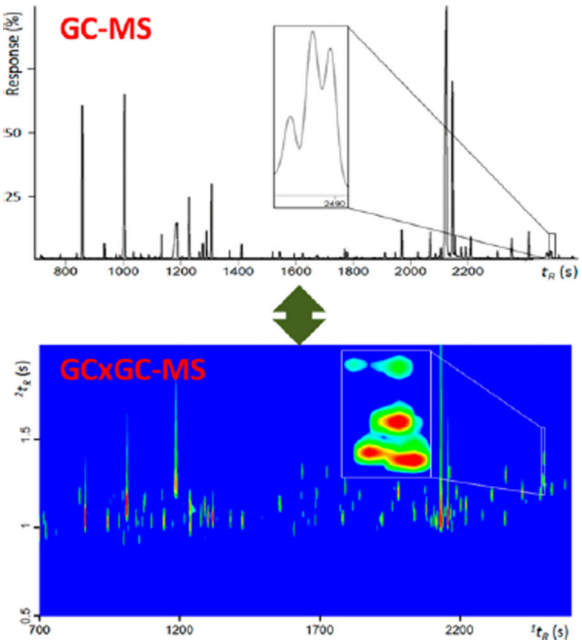

Keywords

biomarker discovery; GC-MS; GC×GC-MS; metabolomics; peak capacity

1. INTRODUCTION

Metabolomics has emerged as one of the latest of the "-omics" disciplines that can detect biomarkers (small molecule metabolites) in biological samples. Metabolites can be polar or nonpolar as well as organic or inorganic. These diverse characteristics make their separation challenging in that there is not a singular instrument capable of analyzing all of these types of molecules. To date, multiple analytical platforms such as liquid chromatography–mass spectrometry (LC-MS), gas chromatography–mass spectrometry (GC-MS), and nuclear magnetic resonance (NMR) spectroscopy have been used in metabolomics for biomarker discovery. Frequently, biological samples are analyzed on both LC-MS and GC-MS platforms to achieve higher metabolite coverage,[1–3] while NMR is generally best suited to quantitatively measure the most abundant metabolites or for structure elucidation.[4,5]

In GC-MS-based metabolomics, metabolites are first separated on a GC column and then subjected to mass spectrometry. Comprehensive two-dimensional gas chromatography mass spectrometry (GC×GC-MS) uses two GC columns, usually connected via a thermal modulator. The second column is typically much shorter than the first (i.e., 1–2 m as opposed to 30–60 m for the first column) with a different stationary phase and is generally operated at a higher temperature. In the case of metabolites that coelute from the first column, the second column may allow for separation due to the different stationary phase as well as the difference in column temperature. Thus, GC×GC-MS can provide superior

chromatographic peak capacity, selectivity, and lower detection limit for the analysis of small molecules. This provides a powerful technique for the analysis of metabolites in complex biological matrixes. Presently, GC×GC-MS has not been widely used for large-scale broad-spectrum biomarker discovery likely due to the increased difficulty of data analysis. New bioinformatics tools have recently emerged that greatly decrease the personnel time necessary to properly process the GC×GC-MS data,[6–8] making this approach feasible for large-scale metabolomics studies.[9,10]

Even though the advantages of GC×GC-MS over GC-MS have been extensively discussed in literature,[11–14] the real-world application of these two analytical platforms for metabolite biomarker discovery in complex biological samples has not been compared in detail. This work examines the performance of GC×GC-MS vs GC-MS for biomarker discovery by analyzing the metabolic profiles of human subjects with a chronic neurodegenerative disorder compared to age-, sex-, and race-matched controls. Metabolite extracts of serum samples from 109 study subjects (54 patients with a chronic neurodegenerative disorder and not currently on medication and 55 controls) were analyzed on both GC×GC-MS and GC-MS platforms. The metabolite extract from a pooled serum sample was used for quality control purposes and was analyzed on both GC×GC-MS and GC-MS platforms after every nine samples. The performance of the GC×GC-MS and GC-MS platforms was then assessed by the number of detected chromatographic peaks, metabolite identification, variations of the aligned peaks in retention times and peak area, and biomarker discovery from the biological samples.

2. EXPERIMENTAL METHODS

Human Serum Samples

The study set included sera from two patient populations: 54 subjects with a chronic neurodegenerative disorder, and 55 sex-, age-, and race-matched controls who were enrolled in the Measurement to Understand Reclassification of Disease of Cabarrus/Kannapolis (MURDOCK) Study and its multiple sclerosis substudy.[15] The samples were stored at −80 °C until sample preparation and subsequent MS analysis.

2.1. Sample Preparation

Samples were extracted by adding 100 μL of serum to 1 mL of ice-cold extraction solvent consisting of methanol/chloroform (v:v = 3:1) containing 10 μg/mL heptadecanoic acid and 10 μg/mL norleucine as internal standards. The samples were briefly vortexed and centrifuged for 15 min at 18 000 rcf at 4 °C. One milliliter of each supernatant was then transferred to a sample vial. The remaining supernatants were combined to generate a pooled quality control (QC) sample. All samples were then dried overnight at room temperature under a gentle flow of N_2.

Dried samples were derivatized using a two-step method. First, 50 μL of freshly prepared methoxyamine in pyridine (20 mg/mL) was added to the samples which were then put on a heated block shaker for 90 min at 1400 rpm and 30 °C. Next, 50 μL of *N*-methyl-*N*-(trimethylsilyl)trifluoroacetamide (MSTFA) with 1% trimethylchlorosilane (TMCS) was

added to the samples which were then put on a heated block shaker for 60 min at 1400 rpm and 70 °C. Samples were then cooled at −20 °C for approximately 1 h, and an aliquot of each was added to individual GC-MS vials with glass inserts for analysis.

2.2. GC-TOF MS and GC×GC-TOF MS Analysis

All sample analyses were performed on a system consisting of an Agilent 7890A gas chromatograph (Agilent Technologies, Santa Clara, CA) with a Gerstel Multipurpose MPS2 autosampler (Gerstel, Inc., Linthicum, MD) interfaced to a LECO Pegasus time-of-flight mass spectrometer with an electron ionization (EI) source (LECO Corporation, St. Joseph, MI). A 60 m × 0.25 mm ${}^{1}d_{c}$ × 0.25 μm ${}^{1}d_{f}$, DB-5 ms UI GC capillary column (phenyl arylene polymer virtually equivalent to a (5%-phenyl)-methylpolysiloxane) (Agilent Technologies) was used for the GC-MS analysis. For the GC×GC-MS analysis, the primary column was identical to the column used in the GC-MS analysis, while the secondary column was a 1 m × 0.25 mm ${}^{1}d_{c}$ × 0.25 μm ${}^{2}d_{f}$, DB-17 ms ((50%-phenyl)-methylpolysiloxane) (Agilent Technologies) column that was placed inside the secondary GC oven after the dual stage quad-jet thermal modulator. The column operation conditions of the GC-MS and GC×GC-MS were as follows: helium carrier gas at 1.0 mL/min; split/splitless inlet at 250 °C; GC oven temperature program of 60 °C for 1 min and then +5 °C/min to 300 °C, holding for 12 min; a transfer line temperature of 300 °C. The GC-MS was operated under a splitless mode while the GC×GC-MS was operated using a split ratio of 30:1 because of increased chromatographic peak heights due to modulator peak focusing. Parameters specific to GC×GC-MS were as follows: the secondary oven temperature program of +10 °C relative to the primary oven; a modulator period of 2.5 s (0.5 s hot, 0.75 s cold); a modulator temperature program of +20 °C relative to the secondary oven temperature. The parameters used for mass spectrometry for the GC-MS and GC×GC-MS analyses were identical as follows: electron energy of −70 eV; ion source temperature of 230 °C; acquisition delay of 710 s; acquisition rate of 20 spectra/s for GC-MS and 200 spectra/s for GC×GC-MS; mass range of m/z = 45–1000.

One microliter of each sample was injected into the GC-MS and GC×GC-MS platforms for analysis. The randomized sample analysis order was the same for both platforms. Multiple QC sample aliquots were prepared from the single QC sample. The pooled QC samples were then analyzed after every nine patient samples. Two to three injections were made from each individual aliquot while the other QC sample aliquots were kept at −20 °C until ready for analysis. During sample analysis, the sample tray holder was kept at 4 °C and samples were removed from −20 °C storage and placed on the tray holder no earlier than 24 h prior to analysis. The experimental data of the pooled QC samples were used to assess overall reproducibility (sample preparation, GC-MS and GC×GC-MS analysis and data analysis) and to correct for any observed variations. Additionally, an alkane retention index standard (C10–C40) was run at the beginning, middle, and end of the sample runs.

2.3. Data Analysis

The raw instrument data from each of the samples were first reduced to a peak list by LECO ChromaTOF software version 4.50.8.0 (LECO Corporation, St. Joseph, MI) using parameters recommended by the vendor (Table S1, Supporting Information); the

NIST/EPA/NIH Mass Spectral Library 2011 (NIST11), the LECO/Fiehn Metabolomics Library and an in-house library were used as reference libraries for metabolite identification. All peak lists were further analyzed using MetPP software,[6] where peak merging and peak list alignment were carried out using DISCO algorithms,[16] and the retention index (RI) matching was performed using iMatch algorithms[17] with the *p*-value threshold set as $p \leq 0.001$. The *p*-value in iMatch refers to the cumulative probability of empirical distribution of absolute RI deviation calculated from the NIST11 RI database, and a *p*-value threshold of $p \leq 0.001$ is equivalent to an absolute RI window of ±59 RI unites owing to the column used in GC-MS and the first dimension column in GC×GC-MS. Finally, a pairwise two-tailed *t*-test with 1000 sample permutations was used to determine whether a metabolite had a significant abundance difference between sample groups with a probability threshold of $p \leq 0.05$.

3. RESULTS

3.1. Analysis of Pooled QC Samples

The GC-MS instrument provides three pieces of information for each metabolite: retention time (t_R), fragment ions (*m/z*), and peak heights for the fragment ions while the GC×GC-MS instrument data provide an additional piece of information, the second dimension retention time (^2t_R). In both cases, the fragment ion *m/z* and its peak height form the EI mass spectrum of each metabolite. Figure 1 shows two sample chromatograms from a pooled QC sample analyzed by GC-MS and GC×GC-MS. The insets in Figure 1A and 1B show the same portion of the two chromatograms. While only three peaks were detected by GC-MS, five chromatographic peaks were detected from this portion of the chromatogram by GC×GC-MS. The two small peaks not detected by GC-MS were due to their low abundance and overlapping retention time with the other three peaks.

Table 1 lists the number of detected chromatographic peaks from a pooled QC sample analyzed by GC-MS and GC×GC-MS using different signal-to-noise ratio (SNR) thresholds for spectrum deconvolution. After manual verification of the chromatographic peaks, we chose a SNR threshold of ≥50 for analysis. The spectral similarity threshold can significantly affect the number of identified metabolites. A low spectral similarity threshold typically results in a large number of metabolites assigned to the detected chromatographic peaks with a high rate of false positive identifications. By setting the threshold of spectral similarity ≥600,[9,10] 366 metabolite identities were assigned to chromatographic peaks detected in each of the 14 GC-MS data sets with a standard deviation of 22 (i.e., 366 ± 22), while 1117 identities were assigned in each of the 14 GC×GC-MS data sets with a standard deviation of 109 (i.e., 1117 ± 109). Additional data processing parameters are shown in Table S1, Supporting Information.

The chromatographic peaks with initial identifications by mass spectrum matching were further subjected to RI matching to remove potential false positive identifications. Metabolites that had a large RI deviation from database values were removed, while metabolites that had large RI variation among multiple database records or those that did not have RI values in the database were not removed.[17] After RI matching, a total of 362 ± 19 and 1095 ± 105 metabolites were kept in the GC-MS and GC×GC-MS data sets,

respectively. Some of these preserved metabolites were assigned to multiple chromatographic peaks as a result of either incomplete derivatization, the presence of isomers, or false-positive identifications. By excluding the redundant metabolite assignments, 302 ± 16 and 629 ± 44 unique metabolites were identified from the GC-MS and GC×GC-MS data sets, respectively.

Figure 2A shows that 201 metabolites were fully aligned in the GC-MS data set and 378 metabolites were fully aligned in the GC×GC-MS data set. Full alignment refers to metabolites that were detected and correctly aligned in every pooled QC sample (i.e., all 14 pooled QC samples). A total of 340 and 981 metabolites were detected in ≥50% of the GC-MS and GC×GC-MS QC samples, respectively. Overall, a larger number of metabolites were consistently detected from the pooled QC samples by GC×GC-MS compared to GC-MS. Figure 2B shows the distribution of the relative standard deviation (RSD) of the retention times for the GC-MS data and the RSDs of the first dimension retention time (^1t_R) and the second dimension retention time (^2t_R) for the GC×GC-MS data. Compared to the GC×GC-MS data set, the GC-MS data set has a less variation in retention times. Figure 2C shows the distribution of the coefficient of variation (CV) of peak area of the fully aligned peaks. The GC-MS and GC×GC-MS data have similar distributions of peak area variations

3.2. Analysis of Human Serum Samples

By setting the chromatographic peak threshold to SNR ≥ 50, 490 ± 26 and 1571 ± 174 peaks were detected from metabolite extracts of the patient serum samples (n = 109) on the GC-MS and GC×GC-MS platforms, respectively: 348 ± 16 unique metabolites were assigned to these chromatographic peaks detected from the GC-MS data, and 1099 ± 118 unique metabolites were assigned to these chromatographic peaks detected from the GC×GC-MS data. A total of 84 metabolites were fully aligned from the GC-MS data while 182 metabolites were fully aligned from the GC×GC-MS data. These numbers are smaller than those acquired for the pooled QC samples shown in Figure 2A due to the increased biological variation among the patient samples compared to the homogeneous pooled QC samples as well as the much larger sample set. In order to detect metabolite biomarkers from the patient population with a high degree of confidence, metabolites present in less than 50% of samples in a sample group (control or diseased) were not considered for further analysis. Therefore, a total of 254 and 757 metabolites, respectively, were carried forward from the GC-MS and GC×GC-MS data for further analysis.

Figure S1 shows clustering results of the metabolite profiles of all human samples analyzed on GC-MS (Figure S1A, Supporting Information) and GC×GC-MS (Figure S1B, Supporting Information), using partial least-squares discriminant analysis (PLSDA). The patient samples and the control samples do not have significant difference in metabolite profile even though GC×GC-MS data show a small degree of separation between the control samples and the patient samples. The cross validation shows a poor predictive ability of the PLSDA models, with Q^2 values of −0.05 for GC-MS data and 0.13 for GC×GC-MS data (Figures S1C and S1D, Supporting Information).

To study the abundance change of each metabolite between control and patient groups, a pairwise two-tailed t-test with the equal variance was used by setting the threshold of

probability to $p \leq 0.05$, during which sample labels were permutated 1000 times. Tables S2 and S3, Supporting Information, summarize the metabolites that were recognized as potential biomarkers from the GC-MS and GC×GC-MS data, respectively. Details of these metabolite biomarkers including identification, technical verification, association network analysis, pathway analysis, and biological discussion will be reported in a future paper.

4. DISCUSSION

4.1. Analysis of Pooled QC Samples

Figure 1 shows that the extra peak capacity of the second column of the GC×GC-MS system generally allowed for coeluting compounds in the GC-MS platform to be fully resolved. Furthermore, a number of low abundance chromatographic peaks were detected in the GC×GC-MS data even though these peaks do not overlap with any other chromatographic peaks. This demonstrates the improved SNR of the GC×GC-MS system, which is beneficial to the analysis of complex samples that have large concentration differences. This increased SNR is despite the fact that the GC×GC-MS analyses utilized a split ratio of 30:1 while the GC-MS analyses were splitless injections. Such increased SNR in GC×GC-MS is accredited to the focusing of the first dimension column effluent in the modulator and then reinjection into the second column. The analysis time in the second column is relatively fast, resulting in minimal band broadening as a function of time.

Table 1 shows that the number of chromatographic peaks detected (N_d) and the number of chromatographic peaks annotated (N_a) had an inverse relationship to the SNR threshold setting. However, the ratio of N_a/N_d increased with the increase of SNR threshold, indicating that a significant number of low abundance metabolites do not generate high quality mass spectra for metabolite identification in both the GC-MS and GC×GC-MS data. At SNR ≥ 50, the GC×GC-MS platform detected about 3 times the number of chromatographic peaks and identified 3 times the number of metabolites via mass spectral matching compared to the GC-MS platform. With increasing SNR threshold, the difference between the number of detected chromatographic peaks and the number of identified metabolites decreased, showing that more intense chromatographic peaks generally produce higher quality mass spectra for metabolite identification, as expected. Due to the nearly identical column and instrument conditions used in the GC-MS and the first dimension of the GC×GC-MS analyses, the increased number of detected chromatographic peaks can be attributed to the increased selectivity provided by the addition of the second column in the GC×GC-MS system.

By design, all metabolites detected in a given pooled QC sample should, in theory, be detected in all other pooled QC samples with identical values (retention time and peak area). However, in reality, this will generally not be the case due to technical and analytical variations such as unavoidable variations in sample processing/handling (both manual and automated), the environment (both macro- and micro-), instrumental variation, etc. Figure 2A shows that 340 and 981 metabolites were detected in more than 50% of the pooled QC samples by GC-MS and GC×GC-MS, and 201 and 378 metabolites were detected in all 14 pooled QC samples by GC-MS and GC×GC-MS, respectively. Figure 2B shows that all metabolites in the GC-MS data have an RSD ≤ 0.5% in their retention times, while 92% of

metabolites in the GC×GC-MS data have an RSD ≤ 0.5% in ^1t_R and ^2t_R. Compared to the GC-MS data, the larger RSD seen in the ^1t_R of the GC×GC-MS data set is partially due to the modulation period P_M = 2.5 s, during which the eluent from the first dimension column was collected and subjected to the second dimension GC for further separation. Thus, the first dimension retention time ^1t_R of GC×GC-MS changes in steps of 2.5 s, while the retention time for GC-MS analyses is continuous. The large RSD in ^2t_R of the GC×GC-MS spectra is caused by the short column length (i.e., 1 m). We did not observe significant difference on the peak area variations between the GC-MS and GC×GC-MS data. After removal of the chromatographic peaks generated by column bleeding, the distributions of the coefficient of variation (CV) of peak areas of the fully aligned GC-MS and GC×GC-MS data are similar (Figure 2C).

Both the retention time and peak area variations were caused by the instrumental variation as well as unavoidable inaccuracies in spectral deconvolution algorithms used for peak detection. To address these technical variations in metabolite marker discovery, MetPP[6] used the DISCO[16] algorithm for cross sample peak list alignment to identify the chromatographic peaks generated by the same metabolite from different samples. Next, contrast normalization was used to minimize the peak area variation between samples. Figure 2C shows that the contrast normalization method can reduce the cross-sample peak area variation for both the GC-MS and GC×GC-MS data sets. Contrast normalization is a nonlinear normalization procedure using smooth curves aimed for normalizing peak intensities, by fitting a smooth curve in scatter plots with the peak intensity differences on the *y*-axis and the intensity means on the *x*-axis after log transformation of the intensities.[18]

While data analysis methods can minimize technical variation after spectrum deconvolution, it is critical to continue developing more accurate spectral deconvolution methods for analysis of both GC-MS and GC×GC-MS data. From our experience, the existing software package, while good, has limitations in accuracy when quantifying low abundance chromatographic peaks and can generate multiple peak entries for one metabolite. The current spectral deconvolution methods can be improved in many ways, including finding the best configuration for peak merging,[19] developing data-dependent chromatographic peak models for peak fitting,[20] etc.

4.2. Analysis of Human Serum Samples

After contrast normalization, a total of 23 metabolites were detected with statistically different abundance levels between the two sample groups in the GC-MS data set (Table S2, Supporting Information), while 34 metabolites in the GC×GC-MS data set (Table S3, Supporting Information) had statistically significant differences in abundance between the two groups. Nine differentially expressed metabolites were detected in both the GC-MS and GC×GC-MS data sets (see metabolites 1–9 in Tables S1 and S2, respectively). All nine of these metabolites had the same direction of change (up- or down-regulated in the patient group) and similar magnitude of fold-change between the control and patient sample groups, demonstrating the robustness of using GC-MS and GC×GC-MS for disease biomarker discovery. For example, Figure S2, Supporting Information, shows abundance changes of the

metabolite 5 between the control and the patient samples; there is a 1.18 fold change with $p = 0.018$ in the GC-MS data, and 1.17 fold change in the GC×GC-MS data with $p = 0.022$.

Of the remaining 14 metabolites that had differences in abundance levels in the GC-MS data set (Table S2, Supporting Information), 10 (rows 10–19) were in the final aligned GC×GC-MS data set, though the differential expression of these were not determined to be statistically significant. This left four metabolites observed by GC-MS with different levels of abundance that were not detected in the GC×GC-MS data set. Two metabolites (rows 20 and 21) were in the original aligned GC×GC-MS data set but were filtered out due to either large RSD in the pooled QC samples or large concentrations in the solvent blank samples. The last two metabolites (rows 22 and 23) were not in the aligned GC×GC-MS data set. It appears that these two peaks may be misidentifications, but it is unclear what the true identifications of the compounds are.

There were 34 metabolites in the GC×GC-MS data set that had significant expression between the two groups (Table S3, Supporting Information). As mentioned above, nine metabolites (rows 1–9) were in the GC-MS significantly differentially expressed data set, twelve (rows 10–22) were in the final aligned GC-MS data set but were not determined to be significantly differentially expressed, and two (rows 23 and 24) were in the original aligned GC-MS data set but were filtered out due to either large RSD in the pooled QC samples, or large concentrations in the solvent blank samples. The last ten metabolites (rows 25–34) were not accounted for in the GC-MS data set. Of these, five were found in some of the GC-MS spectra, but coeluted with other peaks, leading to poor peak deconvolution, which was not the case in the GC×GC-MS spectra. Of the remaining five metabolites, four of them were detected in some of the GC-MS samples, but at extremely low SNR, and thus were not reliably detected by ChromaTOF.

Several factors contribute to the increased number of biomarkers discovered by GC×GC-MS opposed to GC-MS. Compared with the GC×GC-MS platform, the limited separating power of the GC-MS platform affects the accuracy of measuring the abundance of each metabolite and therefore can induce false positive discovery of metabolite biomarkers. For example, Figure 3 shows the DL-phenylalanine peak for both GC-MS and GC×GC-MS runs of the same sample. Both the GC-MS and GC×GC-MS data show that three other metabolites overlap with this metabolite in the retention time in the first dimension (Figure 3A and 3B). The three other metabolites were identified as L-threonic acid, L-cysteine, and creatine from both the GC-MS and GC×GC-MS data (Figure 3C). Even though different split modes were applied in GC-MS and GC×GC-MS, the peak area ratios of these metabolites R_{PA} calculated from the GC-MS and GC×GC-MS data are expected to be consistent. This is true in cases of L-cysteine and creatine, whose peak area ratio between GC-MS and GC×GC-MS was 9.28 and 8.35, respectively. However, the peak area of L-threonic acid was decreased and the peak area of DL-phenylalanine was increased during the deconvolution of GC-MS data, resulting in a significant increase of the peak area ratio of DL-phenylalanine ($R_{PA} = 31.1$) and the decrease of peak area ratio of L-threonic acid ($R_{PA} = 4.01$). Such peak area variation introduced during spectrum deconvolution resulted in phenylalanine being falsely detected as a potential biomarker from the GC-MS data.

The GC-MS analysis used splitless injections, and the GC×GC-MS analysis used a split injection at a ratio of 30:1. The other GC-MS methods employed in this study was simply a mirror of the setup used for GC×GC-MS analysis. Furthermore, identical parameters, such as the SNR threshold, were used to process the GC-MS and GC×GC-MS. While this experimental design and consistent data analysis parameters make direct comparison possible, it is possible that the GC-MS data acquisition parameters can be improved upon. However, we believe that this will not substantially affect our main finding, that GC×GC-MS outperformed GC-MS in the analysis of complex samples such as metabolite extracts from human sera due to increased separating power leading to increased accuracy in spectrum deconvolution which can benefit metabolite biomarker discovery.

5. CONCLUSIONS

It was anticipated that the GC×GC-MS platform would outperform the GC-MS platform in the analysis of complex samples such as metabolite extracts from human sera with a significantly increased number of detected metabolites. This was shown to be the case in the evaluation of serum samples derived from patients with a neurodegenerative disorder compared to age-, sex-, and gender-matched controls. Even though the most abundant metabolites in the pooled QC samples were detected on both the GC-MS and GC×GC-MS platforms, the GC×GC-MS platform detected more chromatographic peaks and identified metabolites. At a threshold of SNR ≥ 50, the GC×GC-MS platform detected 3 times the number of chromatographic peaks relative to the GC-MS platform, with more than 3 times the number of chromatographic peaks being identified. A total of 23 significantly differentially expressed metabolites were detected in the GC-MS data set while 34 metabolites were detected in the GC×GC-MS data set. Among these two groups of metabolites, nine metabolites were detected in both the GC-MS and GC×GC-MS data sets with the same direction of abundance change and similar magnitude of fold-change between the control and patient sample groups, showing a certain degree of consistency using GC-MS and GC×GC-MS for metabolite biomarker discovery. However, the limited resolving power of the GC-MS platform resulted in a large number of metabolites coeluting from the column, introducing a significant challenge for data analysis.

The performance of the GC-MS verse GC×GC-MS in this work showed that more metabolites were found with GC×GC-MS. The experimental conditions were optimized for GC×GC-MS analysis to achieve high metabolite coverage, and the GC-MS methods were simply a mirror of the setup used for GC×GC-MS analysis. The limited accuracy of spectrum deconvolution algorithms and coeluting metabolites in the GC-MS platform are the two major factors contributing to the false discovery of metabolite biomarkers. With the increased peak capacity and sensitivity, more metabolites were detected by GC×GC-MS platform. The metabolite biomarkers only detected in the GC×GC-MS data were either not robustly detected in the GC-MS samples or had large peak area variations because of chromatographic peak overlap. Overall, the GC×GC-MS platform outperformed the GC-MS platform for metabolite biomarker discovery because of its increased resolution, peak capacity, and sensitivity.

Supplementary Material

Refer to Web version on PubMed Central for supplementary material.

Acknowledgments

The authors gratefully acknowledge the support of the Duke MURDOCK Study and its generous participants and the Stone Fund for financial support of sample recruitment. The MURDOCK Study is supported by a gift to Duke University from the David H. Murdock Institute for Business and Culture and grant 1UL1 RR024128-01 from the National Center for Research Resources (NCRR), a component of the National Institutes of Health (NIH) and NIH Roadmap for Medical Research; its contents are solely the responsibility of the authors and do not necessarily represent the official view of NCRR or NIH.

REFERENCES

1. Gao P, Lu C, Zhang F, Sang P, Yang D, Li X, Kong H, Yin P, Tian J, Lu X, Lu A, Xu G. Integrated GC-MS and LC-MS plasma metabonomics analysis of ankylosing spondylitis. Analyst. 2008; 133:1214–1220. [PubMed: 18709197]
2. Klavins K, Drexler H, Hann S, Koellensperger G. Quantitative metabolite profiling utilizing parallel column analysis for simultaneous reversed-phase and hydrophilic interaction liquid chromatography separations combined with tandem mass spectrometry. Anal. Chem. 2014; 86:4145–4150. [PubMed: 24678888]
3. Arbona V, Iglesias DJ, Talon M, Gomez-Cadenas A. Plant phenotype demarcation using nontargeted LC-MS and GC-MS metabolite profiling. J. Agric. Food Chem. 2009; 57:7338–7347. [PubMed: 19639992]
4. Zhang J, Wei S, Liu L, Gowda GAN, Bonney P, Stewart J, Knapp DW, Raftery D. NMR-based metabolomics study of canine bladder cancer. Biochim. Biophys. Acta, Mol. Basis Dis. 2012; 1822:1807–1814.
5. Bingol K, Bruschweiler R. Multidimensional Approaches to NMR-Based Metabolomics. Anal. Chem. 2014; 86:47–57. [PubMed: 24195689]
6. Wei X, Shi X, Koo I, Kim S, Schmidt RH, Arteel GE, Watson WH, McClain C, Zhang X. MetPP: A computational platform for comprehensive two-dimensional gas chromatography time-of-flight mass spectrometry-based metabolomics. Bioinformatics. 2013; 29:1786–1792. [PubMed: 23665844]
7. Castillo S, Mattila I, Miettinen J, Oresic M, Hyotylainen T. Data analysis tool for comprehensive two-dimensional gas chromatography/ time-of-flight mass spectrometry. Anal. Chem. 2011; 83:3058–3067. [PubMed: 21434611]
8. Hoggard JC, Synovec RE. Automated resolution of nontarget analyte signals in GC × GC-TOFMS data using parallel factor analysis. Anal. Chem. 2008; 80:6677–6688. [PubMed: 18672889]
9. Schmidt RH, Jokinen JD, Massey VL, Falkner KC, Shi X, Yin XM, Zhang X, Beier JI, Arteel GE. Olanzapine activates hepatic mammalian target of rapamycin: New mechanistic insight into metabolic dysregulation with atypical antipsychotic drugs. J. Pharmacol. Exp. Ther. 2013; 347:126–135. [PubMed: 23926289]
10. Shi X, Wei X, Koo I, Schmidt RH, Yin X, Vaughn A, Kim SH, McClain CJ, Arteel GE, Zhang X, Watson WH. Metabolomic analysis of the effects of chronic arsenic exposure in a mouse model of diet-induced fatty liver disease. J. Proteome Res. 2014; 13:547–554. [PubMed: 24328084]
11. Wang YW, Chen QA, Norwood DL, McCaffrey J. Recent development in the applications of comprehensive two-dimensional gas chromatograph. J. Liq. Chromatogr. Relat. Technol. 2010; 33:1082–1115.
12. Panic O, Gorecki T. Comprehensive two-dimensional gas chromatography (GC×GC) in environmental analysis and monitoring. Anal. Bioanal. Chem. 2006; 386:1013–1023. [PubMed: 16862380]
13. Dalluge J, Beens J, Brinkman UAT. Comprehensive two-dimensional gas chromatography: a powerful and versatile analytical tool. J. Chromatogr. A. 2003; 1000:69–108. [PubMed: 12877167]

14. Seeley JV, Seeley SK. Multidimensional gas chromatography: Fundamental advances and new applications. Anal. Chem. 2013; 85:557–578. [PubMed: 23137217]
15. Bhattacharya S, Dunham AA, Cornish MA, Christian VA, Ginsburg GS, Tenenbaum JD, Nahm ML, Miranda ML, Califf RM, Dolor RJ, Newby LK. The measurement to understand reclassification of disease of Cabarrus/Kannapolis (MURDOCK) study community registry and biorepository. Am. J. Transl. Res. 2012; 4:458–470. [PubMed: 23145214]
16. Wang B, Fang A, Heim J, Bogdanov B, Pugh S, Libardoni M, Zhang X. DISCO: Distance and spectrum correlation optimization alignment for two-dimensional gas chromatography time-of-flight mass spectrometry-based metabolomics. Anal. Chem. 2010; 82:5069–5081. [PubMed: 20476746]
17. Zhang J, Fang AQ, Wang B, Kim SH, Bogdanov B, Zhou ZX, McClain C, Zhang X. iMatch: A retention index tool for analysis of gas chromatography-mass spectrometry data. J. Chromatogr. A. 2011; 1218:6522–6530. [PubMed: 21813131]
18. Astrand M. Contrast normalization of oligonucleotide arrays. J. Comput. Biol. 2003; 10:95–102. [PubMed: 12676053]
19. Vivo-Truyols G. Bayesian approach for peak detection in twodimensional chromatography. Anal. Chem. 2012; 84:2622–2630. [PubMed: 22229801]
20. Wei X, Shi X, Kim S, S K, Patrick JS, Binkley J, Kong M, McClain C, Zhang X. Data dependent chromatographic peak model-based spectrum deconvolution for analysis of LC-MS data. Anal. Chem. 2014; 86:2156–2165. [PubMed: 24533635]

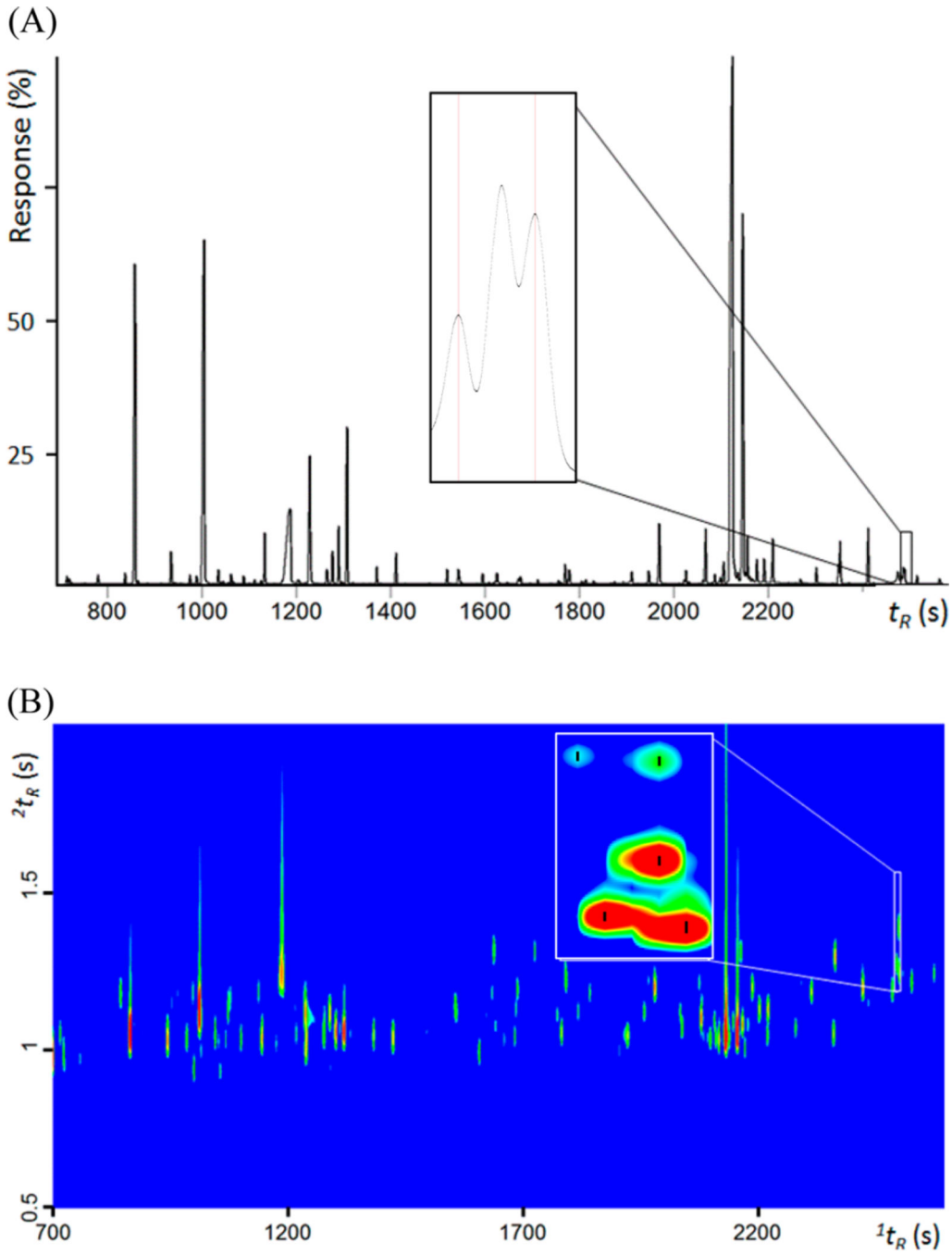

Figure 1.

Separation results of metabolite extract from pooled QC sample on GC-MS and GC×GC-MS, respectively. GC-MS (A) and GC×GC-MS (B) chromatograms are shown. The inset in each figure shows the same portion of the chromatogram in the two main figures, and the vertical bars in each figure insert represents the peak markers detected by ChromaTOF. A total of five chromatographic peaks were detected from this portion of the chromatogram by GC×GC-MS, while only three chromatographic peaks were detected by GC-MS.

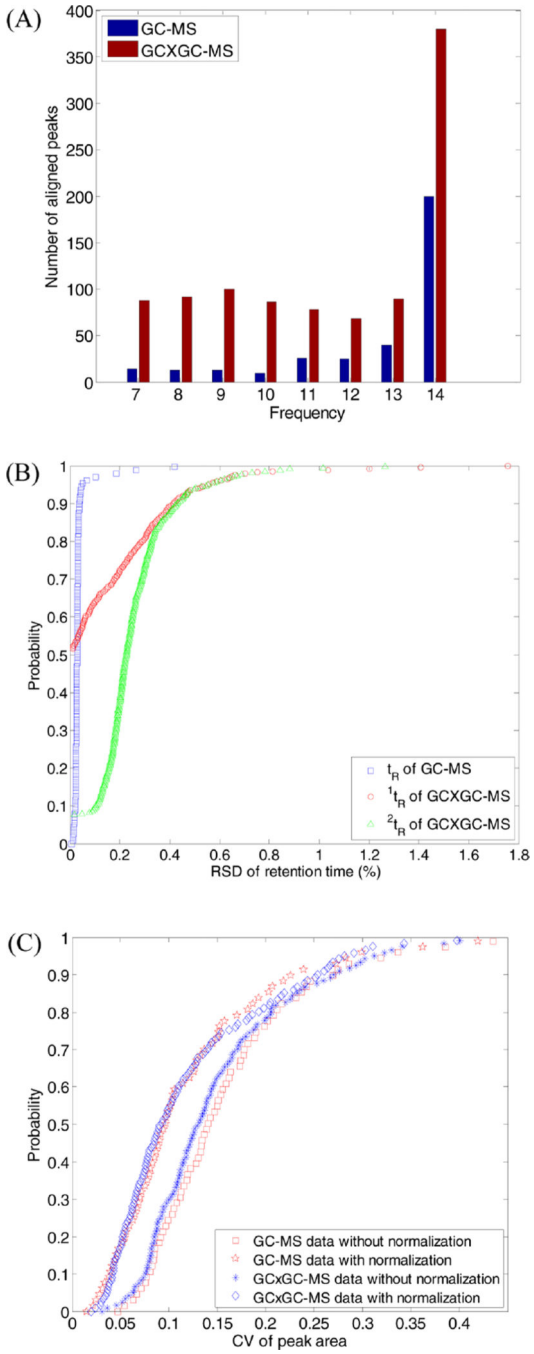

Figure 2.

Variations of analyzing the 14 pooled QC samples on GC-MS and GC×GC-MS platforms. (A)Alignment results of the GC-MS and the GC×GC-MS data. (B) Distribution of the relative standard deviation (RSD) of the retention time (t_R) for the GC-MS data, as well as the relative standard deviation of both the first dimension retention time (^1t_R) and the second dimension retention time (^2t_R) for the GC×GC-MS data. (C) Distributions of coefficient of variation (CV) of peak area before and after normalization.

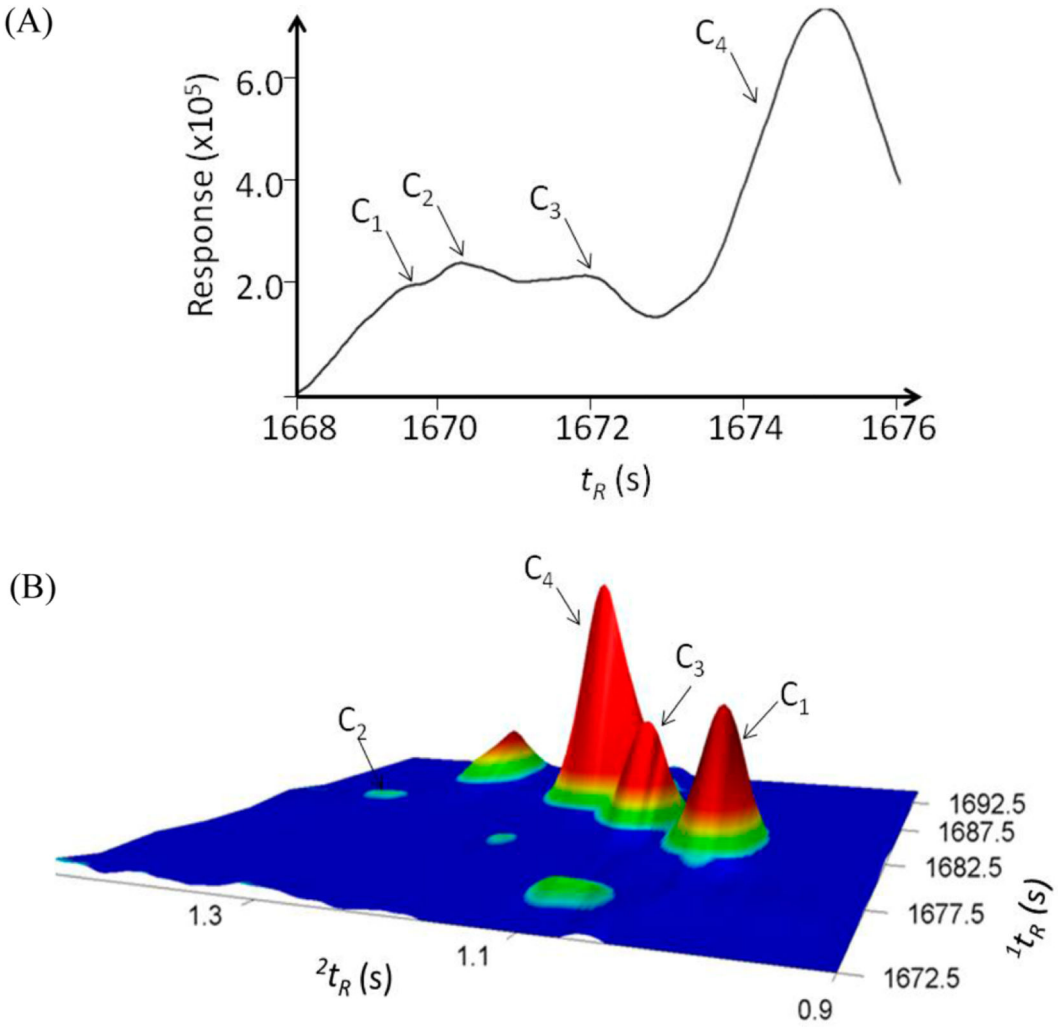

(C)

Metabolites		GC×GC-MS				GC-MS			R_{PA}
ID	Name	^1t_R (s)	^2t_R (s)	Similarity	Area	t_R (s)	Similarity	Area	
C_1	Threonic acid	1682.5	1.035	951	51474	1669.9	919	206444	4.01
C_2	Phenyalanine	1685.0	1.385	859	24273	1670.4	806	760208	31.3
C_3	Cysteine	1685.0	1.115	962	49003	1672.0	949	455018	9.28
C_4	Creatine	1687.5	1.180	951	746036	1675.0	969	6232727	8.35

Figure 3.

Sample spectrum deconvolution in analysis of GC-MS and GC×GC-MS data. A portion of the total ion current chromatogram of a biological sample analyzed on GC-MS (A) and GC×GC-MS (B) are shown. Part C lists the information on deconvoluted metabolite peaks from the GC-MS and the GC×GC-MS data shown in A and B. R_{PA} defined as the ratio of peak area of a metabolite deconvoluted from the GC-MS data divided by that deconvoluted from the GC×GC-MS data.

Table 1

Effect of Signal-to-Noise Ratio on the Spectrum Deconvolution and Metabolite Identification Using Mass Spectral Matching

platform	SNR	no. of peaks detected (N_d)	no. of peaks annotated (N_a)	ratio (N_a/N_d %)
GC-MS	5	968	411	42.5
	10	967	426	44.0
	20	748	404	54.0
	50	505	341	67.5
	100	363	293	80.7
	200	245	219	89.4
	500	148	143	96.6
	1000	109	104	95.4
GC×GC-MS	5	9595	1711	17.8
	10	6737	1623	24.1
	20	3362	1440	42.8
	50	1517	1011	66.6
	100	742	663	89.4
	200	514	479	93.2
	500	301	289	96.0
	1000	156	145	92.9